Short-term volcano-tectonic earthquake forecasts based on a moving Mean-Recurrence-Time algorithm: the El Hierro seismo-volcanic crisis experience

Alicia garcía[1], Servando De la Cruz-Reyna[2,3], José M. Marrero[4,5], and Ramón Ortiz[1]

[1]Institute IGEO, CSIC-UCM. J. Gutierrez Abascal, 2, Madrid 28006, Spain.
[2]Instituto de Geofísica. Universidad Nacional Autónoma de México. C. Universitaria, México D.F. 04510, México.
[3]CUEIV, Universidad de Colima, Colima 28045, México.
[4]Instituto Geofísico. Escuela Politécnica Nacional. Quito, 1701-2759, Ecuador
[5]Unidad de Gestión, Investigación y Desarrollo. Instituto Geofráfico Militar. El Dorado, Quito, 170413, Ecuador.

Correspondence to: Alicia García (alicia.g@igeo.ucm-csic.es)

Abstract. Under certain conditions volcano-tectonic (VT) earthquakes may pose significant hazards to people living in or near active volcanic regions, especially on volcanic islands; however, hazard arising from VT activity caused by localized volcanic sources is rarely addressed in the literature. The evolution of VT earthquakes resulting from a magmatic intrusion shows some orderly behavior that may allow forecasting the occurrence and magnitude of major events. Thus governmental decision-makers can be supplied of warnings of the increased probability of larger-magnitude earthquakes in the short term time-scale. We present here a methodology for forecasting the occurrence of large-magnitude VT events during volcanic crises; it is based on a Mean-Recurrence-Time (MRT) algorithm that translates the Gutenberg-Richter distribution parameter fluctuations into time-windows of increased probability of a major VT earthquake. The MRT forecasting algorithm was developed after observing a repetitive pattern in the seismic swarm episodes occurring between July and November 2011 at El Hierro (Canary Islands). From then on, this methodology has been applied to the consecutive seismic crises registered at El Hierro, achieving a high success rate in the real-time forecasting, within 10 day time-windows, of volcano-tectonic earthquakes

1 Introduction

Volcano-tectonic (VT) earthquakes are considered to be low-magnitude compared to tectonic earthquakes, even though in some cases (three in the 20th century) they have reached M$\geq$7 (Zobin, 2001). Volcanic earthquakes occurring near active subduction zones, which may often reach magnitudes in the range 4-6, rarely cause the same degree of damage or concern among the population that stronger tectonic earthquakes cause. However, in volcanic regions with low tectonic activity,

and consequently with a higher vulnerability to strong ground motions, events exceeding M4 may produce significant damage. Such a situation may become quite serious when that type of VT activity occurs in volcanic islands with unstable topographies, prone to land-slides, as is the case of El Hierro, the westernmost, youngest (< 2 Ma, Ancochea et al, 1994), and smallest (269 km^2) of the
25   Canary Islands.

    In general, earthquake forecasting requires answers to four questions: where, when, how likely and how large? In VT earthquake forecasting, the answer to where is constrained by the extent of the volcanic system. The answer to the second question on timing is related to the onset and evolution of a volcanic crisis. Such crises are generally characterized by VT seismic swarms, lasting an
30   average of 5.5 days in the case of El Hierro, concentrated in regions within or around the volcanic system, and generally defined as "a sequence of events closely clustered in time and space" (Benoit and McNutt, 1996). Since such swarms may include events of damaging magnitudes, it is important to detect the non-random components of the swarm evolution, as it contains factors linking different stages of the process that may allow major VT events to be forecast. We assume that such "causal
35   factors" are related to the nature of the magmatic intrusion process at depth that involves an increasing accumulation of localized stress, which produces the VT earthquake when released. In particular, the magmatic intrusions may produce clustered sources of stress in which pressure increases over relatively short time-scales.

    We picture the situation at El Hierro as voluminous bodies of dense magma intruding into the
40   mantle under the crust from a deeper magma generation region (Martínez-Arevalo et al, 2013). That magma is dense enough to remain in almost isostatic equilibrium at the base of the crust in a process of magmatic underplating (Leahy et al, 2010). As it evolves under the local conditions at mantle-crust boundary depths, the diffusive assimilation of crustal minerals causes an increase in the magma buoyancy over the time-scale of centuries as the assimilation diffusivity is at least one
45   order of magnitude higher than the thermal diffusivity (McLeod and Sparks, 1998; Portnyagin et al, 2008). The increasing buoyancy causes additional stresses and deformations in the overlying crust. Such processes may induce a causative evolution of the seismicity, reflected as an increased rate of seismic energy release, and a changing distribution in the magnitudes of the VT events, as discussed in the following sections. However, at this point, it is important to note that the analysis of such
50   evolution may enable scientists to forecast the occurrence of major VT events in the short-term time scale; nevertheless, in some cases this analysis may not foretell the occurrence of an eruption, as the magma injection and migration process that causes the stress concentration may never reach the surface (Bell and Kilburn, 2012), although an increase in the probability of such an event must be considered. We present next this methodology, developed and used during the El Hierro volcanic
55   process (2011-2015), which is aimed at detecting the precursory behavior of the seismicity before the occurrence of major, potentially damaging, VT earthquakes.

2 El Hierro volcanic process

The morphology of El Hierro island (27.7^o N; 18.0^o W) has been attributed to a triple volcanic rift with the NE, NW and S axes of these rifts diverging by about 120° from each other (Carracedo et al, 1999). The island landscape displays abundant dikes and fissures (Gee et al, 2001), as well as major landslides (Masson et al, 2002). The subaerial island displays a high concentration of volcanoes with a spatial distribution that may be explained by the model proposed by Stroncik et al (2009), in which the volcanic activity at El Hierro is controlled by a complex array of magma pockets. Magma injections from the pockets through dikes or sills may generate VT seismicity.

In July 2011, a sudden increase of seismicity was detected at El Hierro Island, prompting several Spanish institutions to deploy recording instrumentation. In addition to the official seismic network operated by the Instituto Geográfico Nacional (IGN), in September 2011, the IGEO-CSIC Institute (see authors' affiliations) installed, for research purposes, a seismic network consisting of 3 permanent, real-time, vertical, short-period stations, and 5 similar, temporary, manual-access stations. Seismicity, deformations and diffuse gas emissions increased persistently until October 2011, when a submarine eruption at 27° 37.18' N; 17° 59.58' W was first detected (López et al, 2012; Ibáñez et al, 2012; Prates et al, 2013). The eruptive activity persisted for months, until March 2012. However, neither the seismic activity nor the deformations stopped, and have in fact continued to the time of this submission (García et al, 2014b, a).

During the whole episode (2011-2015), only two types of seismicity have been observed: short-period volcano-tectonic (VT) earthquakes, with well-defined P and S phases, and a syn-eruptive long period tremor, patently related to the submarine magma effusion. No long-period (LP) earthquakes have been observed at any time. Here, we analyze the time evolution of the VT earthquakes occurrence rates, as they seem to have similar origins, related to rapid stress concentrations caused by magma intrusions. The VT events do not show significant changes in their waveforms or spectral contents along the duration of the whole episode, as illustrated in Figure 1.

Figure 1 near here

The evolution of the seismic activity at El Hierro island for the whole period of unrest (2011-2015) is summarized in Figure 2, in terms of the time distribution of earthquake magnitudes, the number of earthquakes exceeding M1.5 per day, the cumulative number of events, and the cumulative seismic energy released, estimated from the IGN public earthquake catalog (http://www.ign.es/ign/layoutIn/sismoFormularioCatalogo.do as downloaded on 2015-08-29), and from records of the above-mentioned IGEO-CSIC seismic research network. The uncertainties in calculating the duration and magnitude of very low-amplitude signals recorded by the IGEO-CSIC have been treated according to Del Del Pezzo et al (2003).

Figure 2 near here

Inspection of Figure 2 reveals that the seismicity, deformations and eruption evolution observed during the 2011 unrest episode not only is consistent with the model of Stroncik et al (2009) (Gar-

cía et al, 2014b), but it also reveals some other interesting features of the volcanic unrest process
dynamics. First, as expected, a marked rise of the VT event occurrence rate preceded the onset of
the 10 October 2011 eruption. However, during the continuing seismic unrest, the event rate and
the cumulative number of events have also markedly increased before the occurrence of major VT
earthquakes. But it is the cumulative release of seismic energy, shown in the uppermost plot of
Figure 2, the parameter that best illustrates the precursory character before major VT events. Ad-
ditionally, the M-T diagram in the lower plot of Figure 2 shows a peculiar behavior. The minimum
magnitude rises as the number of higher-magnitude events increases. This may be caused by com-
pleteness fluctuations of the catalog, derived from the difficulties in counting very small events when
larger earthquakes are concurrent, or it may be an actual condition related to the physical process
of seismic energy release. Several other cases in which the completeness is maintained at the lowest
measurable value during the duration of the VT swarm suggest that the latter condition may be real.
For example, Benoit and McNutt (1996) report an increase of the minimum magnitude when the
VT activity approaches a mean magnitude 3. Likewise, De la Cruz-Reyna et al (2008) and Hurst
et al (2014) report a similar behavior for the VT seismicity of Popocatépetl and Tongariro volcanoes
respectively.

To date, five seismo-volcanic crises or VT earthquake swarms have been identified at El Hierro
(García et al, 2014b, a), showing in all cases an increasing trend of the maximum detected magni-
tudes, as shown in Figure 3. It is significant that the acceleration of the seismic energy release rate
begins in all cases when the cumulative seismic energy exceeds the 10^{11}J energy threshold criterion
of Yokoyama (1988). Hours to days after the onset of this acceleration stage, the swarm sequences
culminated with earthquakes exceeding magnitude 4 (Figure 4). Currently, VT earthquake swarms
are classified according to three family types proposed by Benoit and McNutt (1996), and later up-
dated by Farrell et al (2009) and Brumbaugh et al (2014): Type A- mainshock and aftershocks; type
B- foreshocks, mainshock and aftershocks; and type C- swarms without a mainshock. Further exam-
ination of the lower part of Figure 3 reveals that the evolution of the daily rate of seismicity does not
correspond to any of these established earthquake families. We thus introduce a fourth family, type
D, characterized by an increasing number of growing magnitude foreshock events culminating with
a mainshock and followed by a rapid decay of seismicity lasting just a few hours. The differences
between these models are illustrated in Figure 5. Therefore, a type D sequence does not follows
an ETAS model (Ogata, 1992), nor follows the Omori law (Utsu and Ogata, 1995), but it reveals a
causal process that allows forecasting of major VT events.

Figure 3 near here

Figure 4 near here

Figure 5 near here

2.1 Forecasting major VT earthquakes at El Hierro

130 In a time-evolving seismicity, the Gutenberg-Richter Law (GRL, Gutenberg and Richter, 1944) scales the activity, with respect to its magnitude, as:

Equation 1 here

where $N(M)/\Delta T$ is the number of earthquakes with magnitude *M* or larger detected within a given region, in a time interval ΔT. In a process that remains stationary over ΔT, the Gutenberg-

135 Richter Parameters (GRP) *a* and *b* remain constant. Here, we use the time-dependent GRP to estimate the Mean-Recurrence-Time (MRT) of volcanic earthquakes having or exceeding given magnitudes, and thus the likelihood of major events occurring in the shorter time-scale (hours to days). The MRT (t_T) between events with magnitude equal or greater than *M* may thus be estimated from Equation 1 as:

140 **Equation 2 here**

Increasing likelihood of major events may thus be estimated from the increasing rates of occurrence of smaller earthquakes. In practice this may prove to be a difficult task since the available seismic catalogs frequently present completeness uncertainties derived from technical factors such as the stability of the seismic networks and links, weather conditions, background noise, event count-

145 ing and magnitude assignment routines, among others. Problems of catalog completeness in general mean an under-counting of the lowest magnitudes (Bell and Kilburn, 2012) that define a low-end Magnitude Cutoff (MC) above which the GRL holds. A second major problem is that the evolution of VT seismicity in the El Hierro crisis is highly variable, and the estimates for the GRL parameters may vary in time and space, causing local distributions of shocks quite different from those of the full

150 catalog. This problem has been amply discussed in the literature about seismicity from different origins (e.g. Wiemer et al, 1998; Lombardi, 2003; Marzocchi and Sandri, 2003; Helmstetter et al, 2007; Bengoubou-Valerius and Gibert, 2013; Alamilla et al, 2015; Márquez-Ramírez et al, 2015). We have addressed those problems considering a moving and variable time-window ΔT in equations 1 and 2. In most cases, an acceleration of the seismicity occurs when the cumulative energy released by a VT

155 swarm reaches a value near the 10^{11}J energy threshold of Yokoyama (1988). Experience has shown that at El Hierro such swarms precede a stage of accelerated seismicity with increasing magnitudes that culminate in major (M>4) VT events.

The MRT algorithm starts a forecast when a swarm of at least 200 earthquakes with M≥1.5 are detected in a time span of 5 days. Then, a completeness magnitude MC is calculated using the

160 Maximum Curvature Method (MCM, Wiemer and Wyss, 2000). The GRL parameters are estimated for each time-window using a Least-squares Regression Estimator (LRE) and/or a Maximum Likelihood Estimator (MLE) (Peishan et al, 2003; Bengoubou-Valerius and Gibert, 2013). If the seismicity rate drops below 200 earthquakes in 5 days, the MRT algorithm would stop running. However, such a situation has never occurred during the El Hierro seismo-volcanic process. In general, the LRE

165 performs better for seismic swarms, as it allows the contribution of the dominant magnitudes of the

5

swarm to be emphasized underscoring only the linear part of the distribution. In successive swarms, some patterns appear as the time to a mainshock approaches: MC may increase from the initial 1.5 to as much as 3 or more, and the time window shortens. Algorithm 1 shows a schematic description (pseudocode) of the algorithm. The algorithm has been implemented in a batch processing mode that may be activated every 24, 12 or 6 hours, depending on the level of activity.

Algorithm 1 near here

Table 1 shows the main features of the swarms detected at El Hierro, and Figure 6 shows the evolution of the MRT for the initial four cycles of El Hierro activity. A warning window for the likely occurrence of an earthquake exceeding M4 is issued when the calculated MRT for that magnitude drops below 10 days, and a statement saying that there is an increased likelihood of an M4 (or higher) earthquake in the following 10 days is delivered to the decision-makers. The warning remains active until the MRT returns to a value exceeding 10 days. This method has been incorporated into a Volcanic Alert System, (described in García et al, 2014a), where the continuous evolution of the MRT over the whole unrest process is described.

Figure 6 near here

Table 1 near here

An 8-month lull followed those four cycles, and as frequently happens, a belief that the seismo-volcanic crisis had ended spread throughout the island's population. Additional factors, such as a particularly strong winter storm and the Christmas holidays, caused failures of the IGN official seismic network that translated into a rather incomplete seismic catalog. When a new seismic swarm began on 2013-12-20, the MRT could only be calculated using predominantly data from the IGEO-CSIC seismic research network. Figure 7 shows the MRT evolution using magnitudes from both catalogs. On 2013-12-24 a new warning was issued communicating to decision-makers the increased likelihood of a M5 or larger earthquake occurring in the following days. On 2013-12-27, at 17:46:02 UTC, the largest earthquake of the entire episode, with magnitude 5.4, caused numerous landslides across the island, fortunately without casualties. It is interesting to note that no M4 earthquakes occurred in this stage.

Figure 7 near here

3   Discussion and Conclusions

Earthquake forecasting is a problem that has been addressed in the past from various different perspectives. Significant advances were obtained after the introduction of complexity theory (Lorenz, 1963; Mandelbrot, 1977) and the development of predictive algorithms (Gabrielov et al, 1986; Molchan, 1990; Keilis-Borok, 1996; Turcotte, 1997). Currently, the need to implement operational short-term earthquake forecasting based on predictive and forecasting algorithms has been stated by Jordan et al (2011). The MRT is one of such algorithms, based on a property that is typical of

complex systems: seismic events cluster according to a simple scaling law, the Gutenberg-Richter relationship (Equation 1). This empirical relationship contains information about the occurrence of large magnitudes embedded in the number of small-magnitude events (Helmstetter et al, 2007), and the time variations of the distribution of the small-magnitude events provides information about the time-scale of large-magnitude occurrences. In the case of VT earthquakes, two additional factors help to simplify the forecasting process: one is the limited geographic extent of the volcanic source of seismicity, confining the spatial extension of the forecast. The other factor is the short time-scale, measured in days, at which orderly fluctuations of the GRPs evolve reflecting stress accumulations induced by the magma injections, and allowing rapid recognition of significant changes of the MRT as defined in Equation 2, and therefore viable short-term forecasts (García et al, 2014a). In contrast, a similar method for tectonic earthquakes would require recognizing orderly evolution patterns of the GRPs over times scales of years to decades, making short-term forecasting non-viable (e.g. Jordan et al, 2011).

We envision the El Hierro process as the result of magma injections causing rapid stress concentrations capable of triggering seismic swarms. Such swarms culminate with mainshocks that release stress concentrations, and are thus not followed by aftershock sequences. Further magma migrations cause new swarms and mainshocks, in repeating, but non-periodic cycles of activity. For example, the largest earthquakes of the March and December 2013 swarms (see Table 1), were located at less than 20 km West from the westernmost shore of the island, suggesting a nearby localized stress source possibly resulting from subsurface magma injections under that region (Figure 8). From the initial stage of unrest in July 2011, five earthquake swarm cycles have been identified, but only the first of these culminated in an eruption. The subsequent cycles show two main features: first, the swarms are separated by increasingly longer lull intervals, and second, they tend to culminate in mainshocks of increasing magnitudes (see Figure 3).

Figure 8 near here

The forecasting algorithm we are proposing here is based on the above-mentioned envisioning of the process that is causing the seismic swarms, and begins when the background seismic energy exceeds the 10^{11}J energy threshold criterion of Yokoyama (1988). The acceleration of the earthquake rate (Figure 5-D) is interpreted in terms of piecewise estimations of the Gutenberg Richter parameters. The variations of those parameters are, in turn, translated as time-windows of increased likelihood of a large-magnitude earthquake. The MRT algorithm may be, and has been, used in real time. It took the initial VT swarm crises to interpret the process and to recognize and develop the procedures and set the parameters of the MRT algorithm, which was first tested during the third crisis, when a significant reduction of the MRT was detected on 2012-06-05. A M4.2 VT earthquake occurred on 2012-07-03. From then on, the MRT algorithm run continuously in the background. It was not until the fourth crisis that a formal warning was issued on 2013-03-26 communicating to the island authorities and to the Civil Protection officials the increased probability of a M5 earthquake

7

for the following 8 days, as described in García et al (2014a). On 2013-03-31 a M4.9 occurred. In the next volcano-tectonic seismic crisis another formal warning was issued on 2013-12-22, communicating the increased probability of an earthquake exceeding M5 in the next 15 days. Further formal warnings were issued daily afterwards also indicating the increased probability of land slides and other eruption. On 2013-12-27, an M5.4 caused numerous landslides (García et al, 2014a).

In the absence of swarms, the GRPs are calculated with a long database of the seismic catalog, and updated on a daily basis (Algorithm 1), usually yielding fluctuating, but always very long values of the MRT (that may exceed 106 days). At the onset of a seismic swarm, the MRT drops rapidly to values of the order of 103 days. When this happens the GRPs are calculated from shorter time-windows of variable duration, provided that they contain a large enough number of events (at least 200) to yield stable values of the GRPs. When the MRT for events of magnitude 4 or higher is less than 10 days, a warning is issued to the decision makers, expressed as a 10-day window of increased likelihood for larger, potentially damaging earthquakes. Up to the time of this submission, all the recent earthquakes of M$\geq$4 at El Hierro have been forecasted several days in advance. Application of the MRT to other volcanoes may be relatively simple to implement, provided that the observed seismicity corresponds to swarms of type D (Figure 5): increasing number of VT events with increasing magnitudes followed by a mainshock, and by a rapid decay of the seismicity afterwards. The algorithm may be readily adapted to any real-time monitoring system. In addition, the concept of time-windows for the increased likelihood of a large-magnitude earthquake should be easily understood and accepted by governmental decision-makers, making the management of risk more effective.

265 **References**

Alamilla JL, Vai R, Esteva L (2015) Completeness assessment of earthquake catalogues under uncertain knowl-edge. J Seismolog 19(1):27–40, doi:10.1007/s10950-014-9448-x

Ancochea E, Hernán F, Cendrero A, Cantagrel JM, Fúster JM, Ibarrola E, Coello J (1994) Constructive and destructive episodes in the building of a young Oceanic Island, La Palma, Canary Islands, and genesis of the
270 Caldera de Taburiente. J Volcanol Geotherm Res 60(3-4):243–262, doi:10.1016/0377-0273(94)90054-X

Bell AF, Kilburn CR (2012) Precursors to dyke-fed eruptions at basaltic volcanoes: insights from patterns of volcano-tectonic seismicity at Kilauea volcano, Hawaii. Bull Volcanol 74(2):325–339, doi:10.1007/s00445-011-0519-3

Bengoubou-Valerius M, Gibert D (2013) Bootstrap determination of the reliability of b-values: an assessment
275 of statistical estimators with synthetic magnitude series. Nat Hazards 65(1):443–459, doi:10.1007/s11069-012-0376-1

Benoit JP, McNutt SR (1996) Global volcanic earthquake swarm database 1979-1989. Open-file report 96-69, US Department of the Interior, US Gological Survey

Brumbaugh D, Hodge B, Linville L, Cohen A (2014) Analysis of the 2009 earthquake swarm near Sunset Crater
280 volcano, Arizona. J Volcanol Geotherm Res 285:18–28, doi:10.1016/j.jvolgeores.2014.07.016

Carracedo JC, Day SJ, Guillou H, Pérez-Torrado FJ (1999) Giant Quaternary landslides in the evolution of La Palma and El Hierro, Canary Islands. J Volcanol Geotherm Res 94:169–190, doi:10.1016/S0377-0273(99)00102-X

De la Cruz-Reyna S, Yokoyama I, Martinez-Bringas A, Ramos E (2008) Precursory seismicity of the 1994
285 eruption of Popocatepetl Volcano, Central Mexico. Bull Volcanol 70(6):753–767, doi:doi:10.1007/s00445-008-0195-0

Del Pezzo E, Bianco F, Saccorotti G (2003) Duration magnitude uncertainty due to seismic noise: inferences on the temporal pattern of GR b-value at Mt. Vesuvius, Italy. Bull Seismol Soc Am 93(4):1847–1853, doi:10.1785/0120020222

290 Farrell J, Husen S, Smith RB (2009) Earthquake swarm and b-value characterization of the Yellowstone volcano-tectonic system. J Volcanol Geotherm Res 188(1):260–276, doi:10.1016/j.jvolgeores.2009.08.008

Gabrielov A, Dmitrieva O, Keilis-Borok V, Kossobokov V, Kutznetsov I, Levshina T, Mirzoev K, Molchan G, Negmatullaev S, Pisarenko V, Prozorov A, Rinheart W, Rotwain I, Shelbalin P, Shnirman M, Schreider S (1986) Algorithms of long-term earthquakes' prediction, international school on research oriented to earth-
295 quake prediction–algorithms, software and data handling edn. Centro Regional de Sismología para América del Sur, Lima, Peru

García A, Berrocoso M, Marrero JM, Fernández-Ros A, Prates G, De la Cruz-Reyna S, Ortiz R (2014a) Vol-canic alert system (VAS) developed during the 2011-2014 El Hierro (Canary Islands) volcanic process. Bull Volcanol 76:825, doi:10.1007/s00445-014-0825-7

300 García A, Fernández-Ros A, Berrocoso M, Marrero J, Prates G, De la Cruz-Reyna S, Ortiz R (2014b) Magma displacements under insular volcanic fields, applications to eruption forecasting: El Hierro, Canary Islands, 2011?2013. Geophys J Int 196:1–13, doi:10.1093/gji/ggt505

Gee MJ, Watts AB, Masson DG, Mitchell NC (2001) Landslides and the evolution of El Hierro in the Canary Islands. Mar Geol 177(3-4):271–293

305 Gutenberg B, Richter CF (1944) Frequency of earthquakes in California. B Seismol Soc Am 34:185–188

Helmstetter A, Kagan YY, Jackson DD (2007) High-resolution time-independent grid-based forecast for M 5 earthquakes in California. Seismological Research Letters 78(1):78–86, doi:10.1785/gssrl.78.1.78

Hurst T, Jolly AD, Sherburn S (2014) Precursory characteristics of the seismicity before the 6 August 2012 eruption of Tongariro volcano, North Island, New Zealand. J Volcanol Geotherm Res 286:294–302,
310 doi:10.1016/j.jvolgeores.2014.03.004

Ibáñez JM, De Angelis S, Díaz-Moreno A, Hernández P, Alguacil G, Posadas A, Pérez N (2012) Insights into the 2011-2012 submarine eruption off the coast of El Hierro (Canary Islands, Spain) from statistical analyses of earthquake activity. Geophys J Int 191(2):659–670, doi:10.1111/j.1365-246X.2012.05629.x

Jordan TH, Chen YT, Gasparini P, Madariaga R, Main I, Marzocchi W, Papadopoulos G, Sobolev G, Yamaoka
315 K, Zschau J (2011) Operational Earthquake Forecasting. State of Knowledge and Guidelines for Utilization. Ann Geophys-Italy 54(4):315–391, doi:10.4401/ag-5350

Keilis-Borok V (1996) Intermediate-term earthquake prediction. Proc Natl Acad Sci USA 93(9):3748–3755

Leahy GM, Collins JA, Wolfe CJ, Laske G, Solomon SC (2010) Underplating of the Hawaiian Swell: evidence from teleseismic receiver functions. Geophys J Int 183(1):313–329, doi:10.1111/j.1365-246X.2010.04720.x

320 Lombardi AM (2003) The maximum likelihood estimator of b-value for mainshocks. Bull Seismol Soc Am 93(5):2082–2088, doi:10.1785/0120020163

López C, Blanco MJ, Abella R, Brenes B, Rodríguez-Cabrera VM, Casas B, Cerdeña ID, Felpeto A, de Villalta F, del Fresno C, García O, García-Arias M, García-Cañada L, Gomis-Moreno A, González-Alonso E, Guzmán-Pérez J, Iribarren I, López-Díaz R, Luengo-Oroz N, Meletlidis S, Moreno M, Moure D, Pereda de
325 Pablo J, Rodero C, Romero E, Sainz-Maza S, Sentre-Domingo M, Torres P, Trigo P, Villasante-Marcos V (2012) Monitoring the volcanic unrest of El Hierro (Canary Islands) before the onset of the 2011-2012 submarine eruption. Geophys Res Lett 39:L13,303, doi:10.1029/2012GL051846

Lorenz EN (1963) Deterministic nonperiodic flow. J Atmos Sci 20(2):130–141

Mandelbrot BB (1977) Fractals: Form, Chance and Dimension. W. H. Freeman and Co.

330 Márquez-Ramírez V, Nava F, Zúñiga F (2015) Correcting the Gutenberg–Richter b-value for effects of rounding and noise. Earthquake Science 28(2):129–134, doi:10.1007/s11589-015-0116-1

Martínez-Arevalo C, Mancilla FdL, Helffrich G, García A (2013) Seismic Evidence of a Regional Sublithospheric Low Velocity Layer beneath the Canary Islands. Tectonophysics 608:586–599, doi:10.1016/j.tecto.2013.08.021

335 Marzocchi W, Sandri L (2003) A review and new insights on the estimation of the b-valueand its uncertainty. Ann Geophys-Italy 46(6):1271–1282

Masson D, Watts A, Gee M, Urgeles R, Mitchell N, Bas TL, Canals M (2002) Slope failures on the flanks of the western Canary Islands. Earth-Sci Rev 57(1-2):1–35

McLeod P, Sparks RSJ (1998) The dynamics of xenolith assimilation. Contrib Mineral Petr 132(1):21–33,
340 doi:10.1007/s004100050402

Molchan G (1990) Strategies in strong earthquake prediction. Phys Earth Planet In 61(1-2):84–98, doi:10.1016/0031-9201(90)90097-H

Ogata Y (1992) Detection of precursory relative quiescence before great earthquakes through a statistical model. J Geophys Res-Sol Ea 97(B13):19,845–19,871, doi:10.1029/92JB00708

345 Peishan C, Tongxia B, Baokun L (2003) The b-Value and Earthquake Occurrence Period. Chinese Journal of Geophysics 46(4):736–749, doi:10.1002/cjg2.3393

Portnyagin M, Almeev R, Matveev S, Holtz F (2008) Experimental evidence for rapid water exchange between melt inclusions in olivine and host magma. Earth Planet Sci Lett 272(3):541–552, doi:10.1016/j.epsl.2008.05.020

350 Prates G, García A, Fernández-Ros A, Marrero JM, Ortiz R, Berrocoso M (2013) Enhancement of sub-daily positioning solutions for surface deformation surveillance at El Hierro volcano (Canary Islands - Spain). Bull Volcanol 75:724, doi:10.1007/s00445-013-0724-3

Stroncik N, Klügel A, Hansteen T (2009) The magmatic plumbing system beneath El Hierro (Canary Islands): constraints from phenocrysts and naturally quenched basaltic glasses in submarine rocks. Contrib Mineral
355 Petr 157:593–607, doi:10.1007/s00410-008-0354-5

Turcotte DL (1997) Fractals and chaos in geology and geophysics. Cambridge University Press

Utsu T, Ogata Y (1995) The centenary of the Omori formula for a decay law of aftershock activity. J Phys Earth 43(1):1–33

Wiemer S, Wyss M (2000) Minimum magnitude of completeness in earthquake catalogs: examples from Alaska,
360 the western United States, and Japan. Bull Seismol Soc Am 90(4):859–869, doi:10.1785/0119990114

Wiemer S, McNutt SR, Wyss M (1998) Temporal and three-dimensional spatial analyses of the frequency–magnitude distribution near Long Valley Caldera, California. Geophys J Int 134(2):409–421, doi:10.1046/j.1365-246x.1998.00561.x

Yokoyama I (1988) Seismic energy releases from volcanoes. Bull Volcanol 50:1–13, doi:10.1007/BF01047504
365 Zobin VM (2001) Seismic hazard of volcanic activity. J Volcanol Geotherm Res 112(1):1–14, doi:10.1016/S0377-0273(01)00230-X

FIGURES
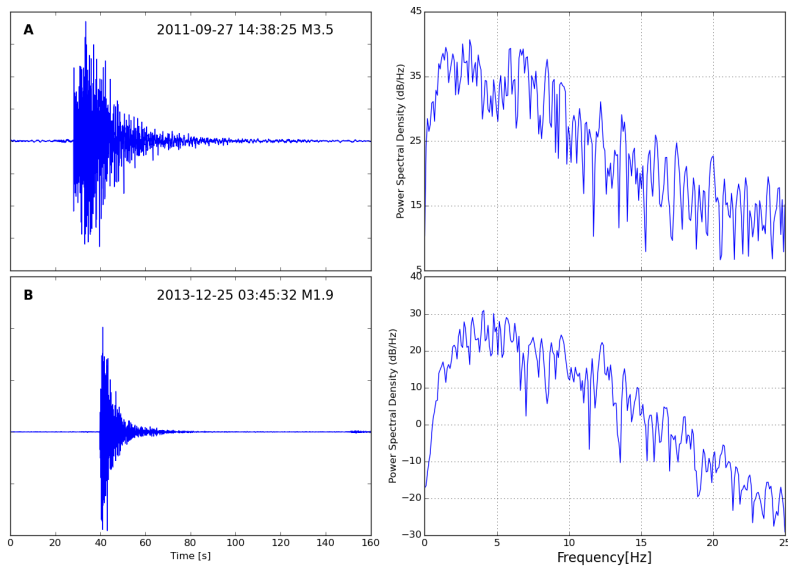
Figure 1. Characteristic VT earthquakes of the El Hierro seismo-volcanic process and their spectra. (A) Event recorded on 2011-09-27, before the eruption, at ~ 6.3 km to the SE of the island center. (B) Event recorded on 2013-12-24, after the eruption at ~ 10.4 km SW of the island center.
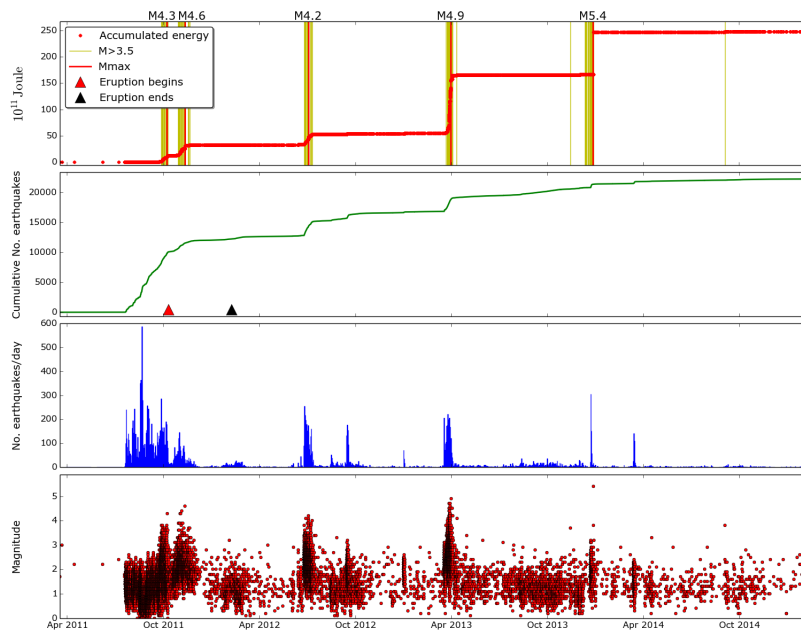
Figure 2. Evolution of the seismic activity at El Hierro Island between 2011-03-18 and 2015-02-12. Data are from the IGN public earthquake catalog and the IGEO-CSIC seismic research network.
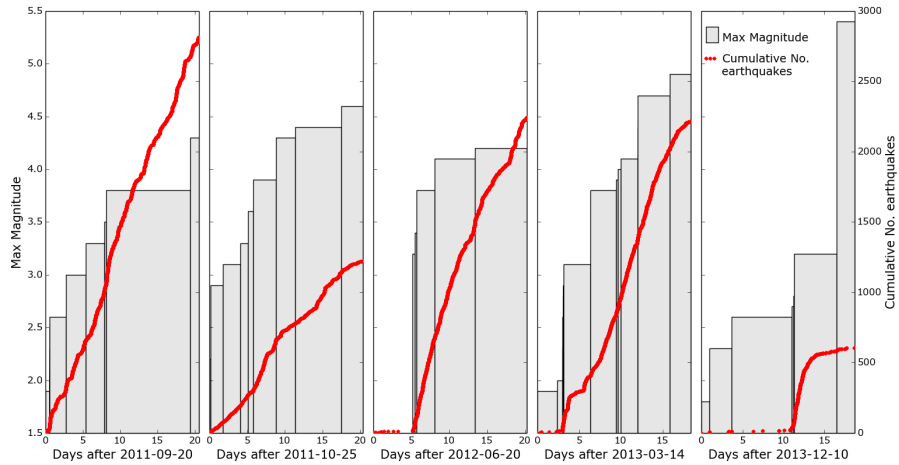
Figure 3. Time evolution of the daily count of VT events (red dots) and maximun magnitudes (gray bars) during the earthquake swarms of the El Hierro seismo-volcanic process.
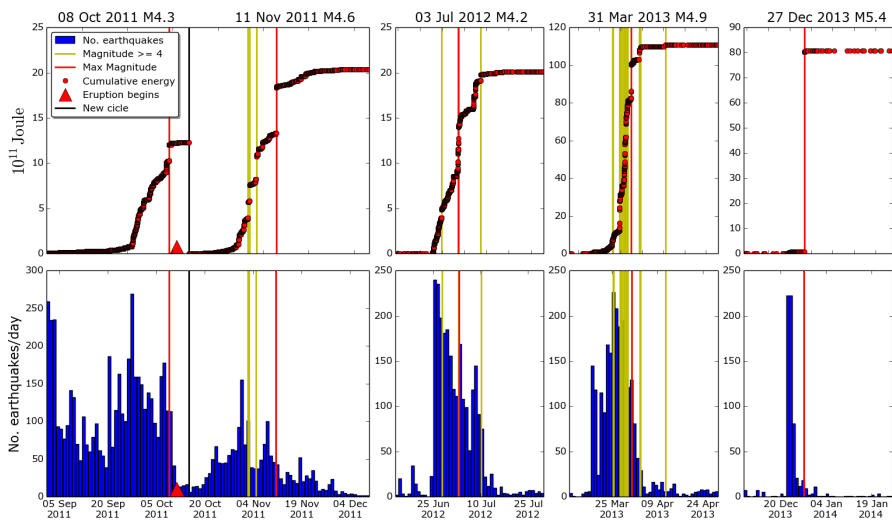
Figure 4. Seismo-volcanic crises identified at El Hierro Island (2011-2014). The upper plots show the evolution of seismic energy for each of the cycles of unrest. The lower plots show the daily event count. The plots illustrate how the seismic activity drops rapidly after the largest magnitude earthquakes. Particularly significant is the absence of aftershocks after the largest (M5.4) earthquake of 2013-12-27. Data are from IGN public earthquake catalog and the IGEO-CSIC seismic research network.

13
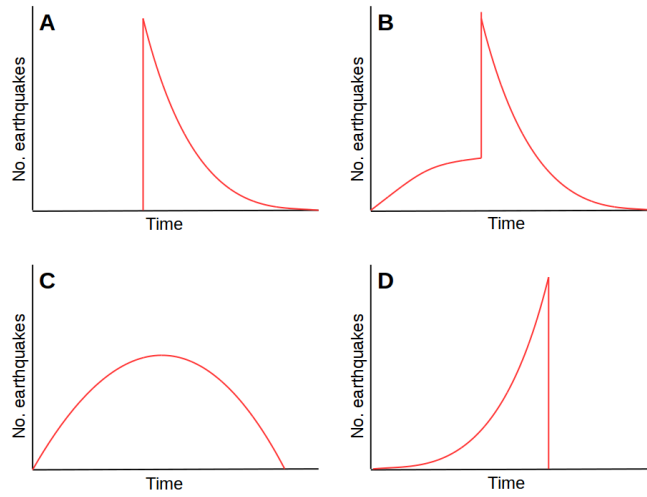
Figure 5. Seismic swarms are usually classified in three family types (A, B, C, Farrell et al, 2009; Brumbaugh et al, 2014). From our results at El Hierro in 2011-2015, we propose a fourth family type D, characterized by an increasing number of VT earthquakes and their magnitudes with time, and by a quick decay of the seismicity, in a matter of hours after a mainshock usually exceeding M4.
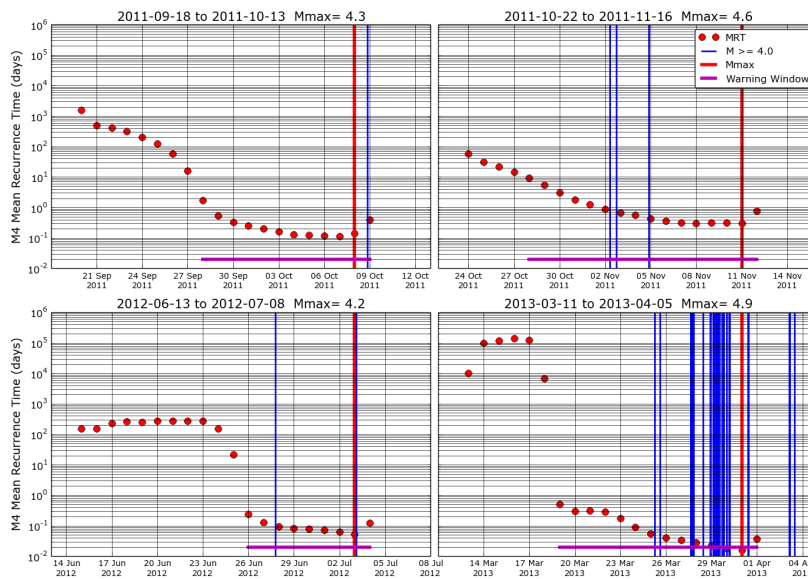
Figure 6. MRT evolution for four periods: 2011-08-18 to 2011-10-10; 2011-10-22 to 2011-11-13; 2012-06-13 to 2012-07-05; and 2013-03-11 to 2013-04-02. The warning windows were triggered when MRT dropped below 10 days.
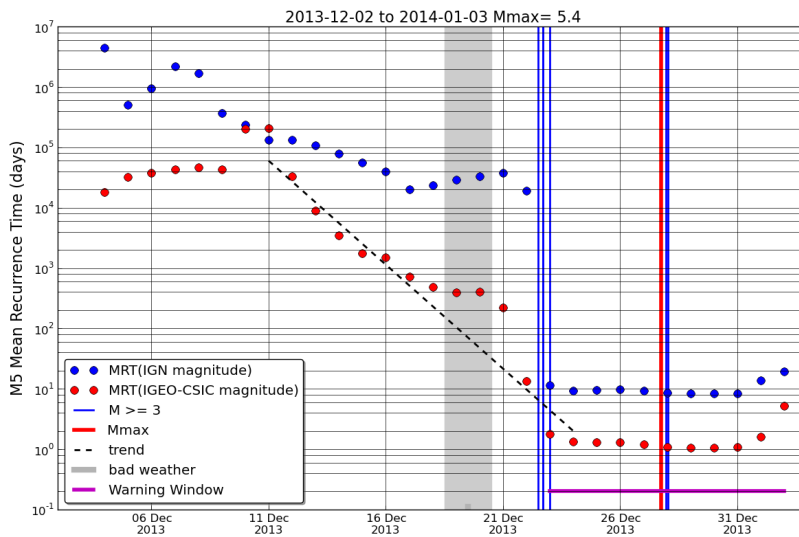
Figure 7. MRT evolution in December 2013 calculated from the IGN official catalog (blue) and from the IGEO-CSIC catalog (red). The magnitude of the earthquake on 2013-12-27 17:46:02 was estimated by IGN as 5.1, and as 5.4 by the IGEO-CSIC network and other international catalogs.
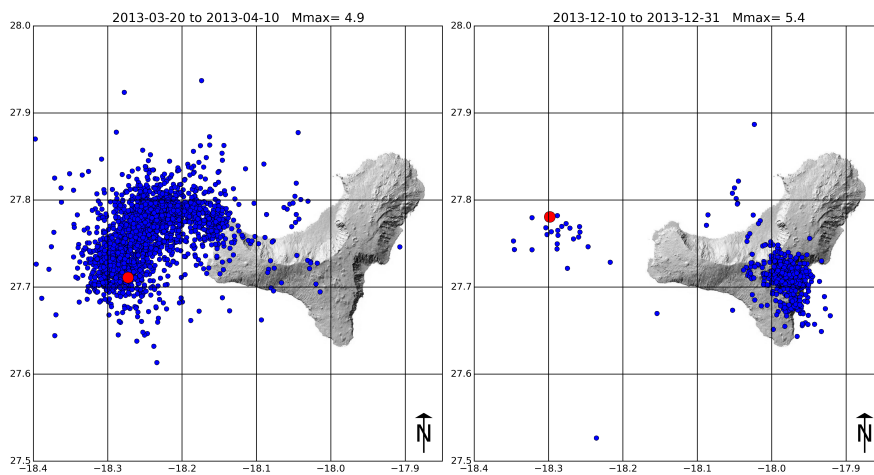
Figure 8. Swarms and mainshock epicentres of the March and December 2013 seismicity cycles. The M5.4 mainshock of 2013-12-27, at 17:46:02 UTC is located in the same region of the March 2013 cycle.

15

TABLES

Table 1. Characteristics of El Hierro swarms.

Mainshock Date	Magnitude		Swarm duration (days)	Number of events
	Mean	Max		
2011-10-08	2.33	4.3	10	934
2011-11-11	2.27	4.6	8	354
2012-07-03	2.35	4.2	5	635
2013-03-31	2.75	4.9	4	651
2013-12-27	2.09	5.4	4	466

EQUATIONS

370 $$\log[N(M)/\Delta T] = a - bM \tag{1}$$

$$t_T = \Delta T * 10^{[bM-a]} \tag{2}$$

ALGORITHM

Algorithm 1 Pseudocode of the MRT algorithm developed to forecast mainshocks applied during the El Hierro seismo-volcanic process (2011-2015).

1: *Get seismic catalog* ← `download from IGN website`

2: *Count numer of events* ← `In the last 5 days`

3: **if** *earthquakes M1.5 > 200 events* **then**

4:     *Compute current MC* ← `Magnitude Cutoff, using Maximum`

5:     `Curvature Method (MCM)`

6:     *Compute Time window* ← `Use constant MC`

7:     *Compute number of events where M>MC*

8:     **if** *Number of events (M>MC) > 200 events* **then**

9:         *Select all events where M>MC*

10:         *Compute Gutenberg-Richter Parameters* ← `Using Least-squares`

11:         `Regression Estimator (LRE) and/or`

12:         `Maximum Likelihood Estimator (MLE)`

13:         *Compute Mean-Recurrence-Time (MRT) for M4 events*

14:         **if** *MRT for M4 events < 10 days* **then**

15:             **Activate Warning Window**

16:         **end if**

17:     **end if**

18: **end if**